Preparation and characterization of a novel ZnO/TiO_2 composite catalyst with amorphous/crystalline heterostructure

Tao Zeng*

College of International Education
Mudanjiang Normal University
Mudanjiang
157011, China

Abstract—Semiconductor photocatalysts have recently received great interests owing to their wide applications in environmental purification, solar energy conversion, and water splitting. However, enhancing the photocatalytic efficiency of TiO_2 to meet the practical application requirements is still a challenge because of the bottleneck of the poor quantum yield caused by the rapid recombination of photogenerated electrons and holes. Much effort has been made to increase the electron-hole pair separation efficiency. Here, A novel ZnO/TiO_2 amorphous/crystalline composite catalyst has been prepared by a low-temperature hydrothermal method. Based on the XRD and HRTEM analysis, there are amounts of anatase surrounded by amorphous ZnO when the mole ratio of Zn to Ti is 1/3, which could help improve the photocatalytic activity of the ZnO/TiO_2 amorphous/crystalline composite catalyst. These encouraging finding could be expanded to other system or reactions and could open up a new direction in catalysis.

Keywords-Amorphous/crystalline;composite; Heterostructure; Ti/Zn ratio; Hydrothermal treatment

I. INTRODUCTION

In the past 20 years, designs and controllable fabrications of nanomaterials with heterostructured structures have recently become an increasingly important research branch in materials area, that's because their quantum yields and photoluminescence tend to increase [1-5]. Moreover, various amorphous materials have been prepared and employed in catalysis in the field of heterogeneous catalysis and other area for its novel structures and electronic characters [6-9]. Compared with its crystallized counterpart, a metal in an amorphous state hold many more lattice defects and thus could give birth to distinct effects in mediating the electronic structure or tuning the atomic arrangement [10,11]. Although many studies have been focused on heterostructured ZnO/TiO_2 NPs, coupling TiO_2 with amorphous ZnO to form amorphous ZnO/TiO_2 heterostructured NPs has been rarely reported. Herein, we report a facile route for synthesizing amorphous ZnO/TiO_2 composite NPs in different crystal states. Unexpectedly, in contrast to its crystallized counterpart, ZnO in the amorphous state exerts a distinct and powerful ability for the photocatalytic activity. Thus, the synthesis of amorphous ZnO/TiO_2 composite NPs in different crystal states and a comparison of their catalytic activities are of great interest.

In another side, many studies have reported that amorphous materials have special performance in the field of heterogeneous catalysis and other areas for their novel structures and electronic characters. Cao et al found that amorphous manganese oxide materials as photo-oxidation catalysts were more active regenerable than crystalline manganese oxides or any other oxidic catalysts [12]. Yan et al found that amorphous Fe nanoparticles have high catalytic activity for the generation of H_2. Especially, synergistic effect resulted from the combination of crystalline and amorphous phase will generate surprising effects for improving the catalytic activity and could be used in many fields. For instance, Cui et al designed a silicon crystalline-amorphous core shell nanowires, they found amorphous Si instead of crystalline Si can be selected to be electrochemically active, and the Silicon crystalline-amorphous core shell structure also have a very high charge storage capacity for lithium ion batteries. Zhang et al studied Fe@Pt core-shell NPs and found iron in the amorphous state could result in a high catalytic activity. Chen et al synthesized Fe_3O_4/SnO_2 (amorphous) nanorods and found the nanocomposites exhibiting excellent microwave absorption properties. Meng et al prepared amorphous/crystalline metal oxide-graphene using atomic layer deposition [13-16].

II. EXPERIMENTAL

A. Catalyst preparation

Firstly, 6 ml of tetrabutyl titanate were added into 40ml of ethanol solution under fast and uniform stirring at room temperature as precursors of TiO_2, which denoted as solution A. Secondly, a certain amount of zinc acetate was dissolved in 20ml deionized water under continuous stirring. The molar ratio of ZnO/TiO_2 was 1/1, 1/3 and 1/5, respectively. And then some ammonia water was added

dropwise to this 20mL zinc acetate solution under vigorous stirring until the suspending liquid became clarified, and the mixture was denoted as solution B. The third step is to drop solution B into solution A under vigorous stirring. After being stirred for 2 h, the mixture was transferred to a 100mL Teflon-lined stainless steel autoclave, followed by a hydrothermal treatment at 120 ◦C for 12 h. The samples were denoted as HZT1, HZT3 and HZT5.

B. Characterization techniques

X-ray diffraction (XRD) patterns were collected on a Rigaku D/max-2200VPC diffractometer with CuKa radiation operated at 40 kV and 50 mA. Transmission electron nement microscopy (TEM) and highresolution transmission electron microscopy (HRTEM) images were taken on a JEOL-JEM 2010 field emission gun (FEG) transmission electron microscope working at an accelerating voltage of 200 kV and equipped with a slow scan digital camera. To reveal the crystalline structure, selected area electron diffraction (SAED) and Fourier transform (FT) of the HRTEM images were performed.

III. RESULTS AND DISCUSSION

The crystal structures of the ZnO/TiO_2 composite NPs were also investigated by X-ray diffraction (Fig .1). The XRD patterns of the HZT1 presents a disordered amorphous state, suggesting the ZnO/TiO_2 composite nanoparticles are mixed amorphous, and it is interesting to note the characteristic peak of HZT3 is a kind of amorphous ZnO/TiO_2 composite catalyst. When the Zn/Ti ratio reaches 1/5, the amorphous ZnO has disappear entirely and was replaced by a signature of pure anatase TiO_2 phase, and there is also did not show any characteristic peaks for ZnO crystalline.

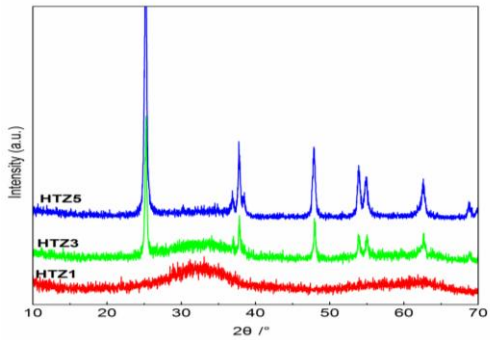

Figure 1. XRD spectra of the prepared prepared samples with different Zn/Ti ratio.

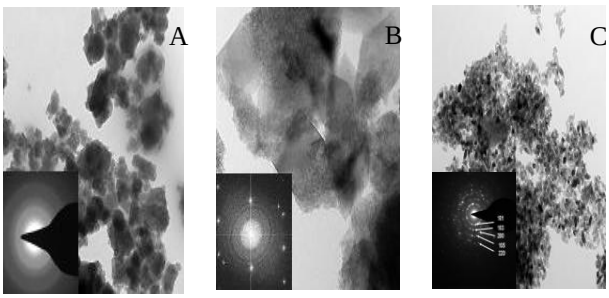

Figure 2. TEM images of (A)HZT1 and SAED inset (B) HZT3 and FT inset (C) HZT5 and SAED inset.

Fig .2 showed the TEM images of the sample (A) HZT1 and SAED inset (B) HZT3 and FT inset (C) HZT5 and SAED inset. From the Fig .2(A), it is self-evidence the as-made ZnO/TiO_2 composite NPs showed an amorphous feature, which is consistent with results from the XRD analysis. From the Fig .2(B), it can be confirmed the HZT3 sample is a kind of amorphous ZnO/TiO_2 composite NPs, which is good agreement with the XRD studies. Fig .2(C) showed the TEM image (SAED inset) of HZT5, obviously, no traces of amorphous ZnO can be found either by TEM image or by SAED pattern, instead only pure anatase nanocrystals can be observed, which is also consistent with the XRD studies.

Fig .3 exhibits the HRTEM image of HZT3 sample. The lattice spacing was about 0.351 nm corresponding to the anatase (101) crystallographic planes. Besides, there are a large number of defects shows on the crystalline structure of HZT3, and some low intensity points on the FT also support the presence of small crystalline defects. The corresponding filtered image clearly shows how the crystal planes are interrupted by extensive defects in its structure. The presence of these lattice defects in the amorphous ZnO/TiO_2 composite NPs may give birth to distinct effects in mediating the electronic structure or tuning the atomic arrangement.

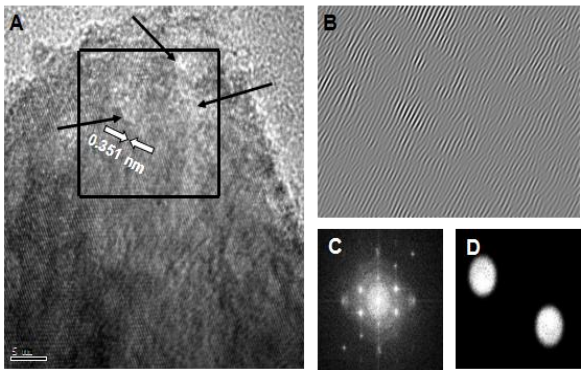

Figure 3. (A) HRTEM image of HZT3 nanoparticle containing extensive crystalline defects; (B) Filtered image from the square area in (A) including the spots of 0.351 nm; (C) FT of the square area in (A); (D) Mask used to reconstruct the image (B).

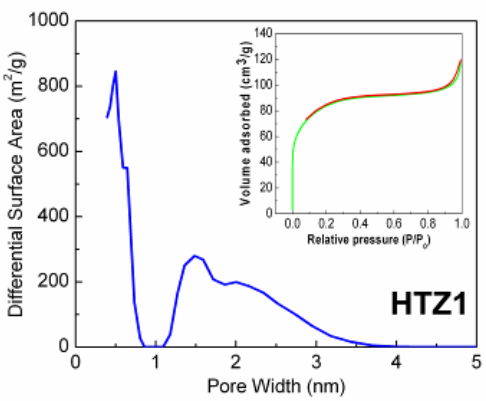

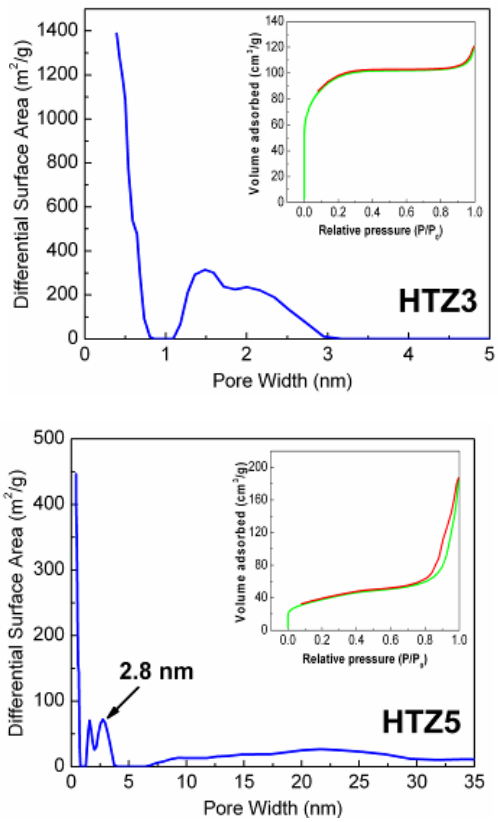

Figure 4. Pore size distributions for HTZ1, HTZ3 and HTZ5 employing DFT method; N_2 adsorption isotherm are shown in respective insets

Table 1 Summary of the physicochemical properties of the HTZ1, HTZ3 and HTZ5

Samples	BET[a] (m^2/g)	micropore area[b] (m^2/g)	Pore size[c] (nm)	Pore volume[d] (cm^3/g)
HTZ1	272.4	105.9	2.7	0.18
HTZ3	311.9	143.3	2.3	0.19
HTZ5	130.1	13.6	8.7	0.29

a Determined by applying Brunauere Emmette Teller (BET) equation

b T-plot Micropore area

c Adsorption average pore width (4V/A by BET)

d Single point adsorption total pore volume of pores at $P/P_0 = 0.99$

The N_2 adsorption/desorption isotherms taken on HTZ1, HTZ3 and HTZ5 samples are shown in Fig .4. Obviously, the isotherms of HTZ1 and HTZ3 could be classified as typical type I isotherm characteristic for the microporous solids. While the N_2 adsorption volume of HTZ3 is higher than that of HTZ1, indicating HTZ3 has a larger micropore area. The isotherms of HTZ5 exhibited Type IV isotherms, indicating the presence of well-developed mesoporosity in the sample. The specific surface areas of each sample, calculated by the multi-point Brunauer- Emmett-Teller (BET) method, are 272.4 m^2/g, 311.9 m^2/g and 130.1 m^2/g for HTZ1, HTZ3 and HTZ5, respectively. And the above analysis coincides with their pore size distributions employing Density functional theory (DFT) method. HTZ1 and HTZ3 exhibited a similar pore size distribution at 0.4-4 nm and 0.38-3 nm respectively, while the HTZ5 showed a broader pore size distribution in the range of 0.4-30 nm. The BET surface area, micropore area, pore size and pore volume are summarized in Table 1.

FTIR study was performed to reveal the changes in the vibrational properties upon different proportions of the ZnO/TiO_2 composite nanoparticles. Fig .5 shows the FTIR spectra of the samples HTZ1, HTZ2, HTZ3 and HTZ5. The broad bands at 3400 cm^{-1} and 1630 cm^{-1} correspond to the surface-adsorbed water and hydroxyl groups. These bands become a little stronger with the increase of the Ti ratio, indicating increased Ti ratio may contribute to increase the surface-adsorbed water and hydroxyl groups of titania. The bands at 1404 cm^{-1} and 1242 cm^{-1} can be assigned to the symmetric stretch of Ti-O bond and Ti-OH bond. The bands around 618 cm^{-1} and 456 cm^{-1} are attributed to the vibration mode of O-Ti-O band corresponding to the crystalline titania in the anatase form.[42] The vibration band belonging to ZnO does not occur in the FTIR spectra.

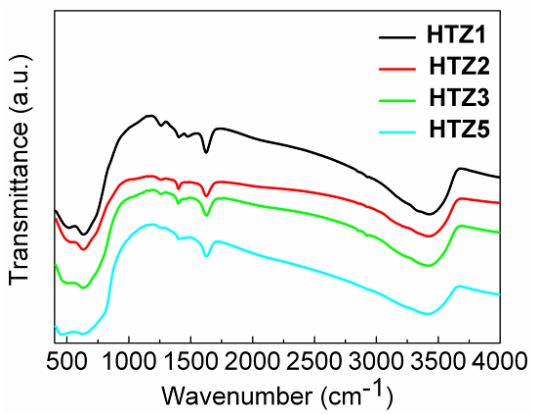

Figure 5. The FTIR spectra of the as-prepared samples.

Compared with its crystallized counterpart, material in amorphous state holds more lattice defects and thus could give birth to distinct effects in mediating the electronic structure or tuning the atomic arrangement. And the combination of amorphous and crystalline will has a high concentration of unsaturated sites, which causes the adsorption and surface reactions much easier than the pure crystalline catalysts. And synergistic effect resulted from the combination of crystalline and amorphous will generate highly active catalytic centers so as to improve the photocatalytic performance. Therefore, the results demonstrate that the nanoparticles with amorphous/crystallite composite structure have the excellent photocatalytic performance compared with the single amorphous or crystalline phase. Similiarly, Bickley and co-workers have reported that Degussa P25 with anatase crystallites with amorphous and rutile phases could show unusually high photocatalytic activity, which is attributed to the complex structure and the localized Anderson states of amorphous TiO_2 that can increase the lifetimes of the electrons/holes pairs and thereby enhance the photocatalytic activity.Besides the advantages of the

amorphous/crystalline composite structure mentioned above, the intrinsic strengths of ZnO/TiO_2 heterostructure also play an important role in separation of photogenerated electron-hole pairs.

Fig .6 shows a configuration model of HTZ3 with amorphous/crystalline composite structure. The high activity of the composite photocatalyst is considered to be due to a fast charge separation. The difference in the positions of conduction bands between ZnO and TiO_2 drives photoelectrons in ZnO to surrounding TiO_2 nanoparticles immediately upon light absorption, thus forcibly separate the pairs of electrons/holes on the surface and reduce their recombination effectively, facilitating the photocatalytic activity of the catalyst. And the surface modifying amorphous ZnO exhibited intimate contact with the base TiO_2 by forming heterostructure which resulted in much easier charge transfer and better separation efficiency. Moreover, HTZ3 also has a large specific surface area (311.9 m^2/g), which provides a large interface for photocatalytic reaction. Homogeneous distribution of amorphous ZnO and enlarged specific surface areas is convenient to obtain effective charge transfer between TiO_2 and ZnO. Furthermore, as confirmed by HRTEM analysis, the large amount of the lattice defects in the surface of the amorphous/crystallite composite structure can provide more active sites for photocatalytic reaction than other samples, which is beneficial to improve the photocatalytic activity. Therefore, an excellent catalytic effect could be expected for catalysts composed of the mixture of amorphous and crystalline structure.

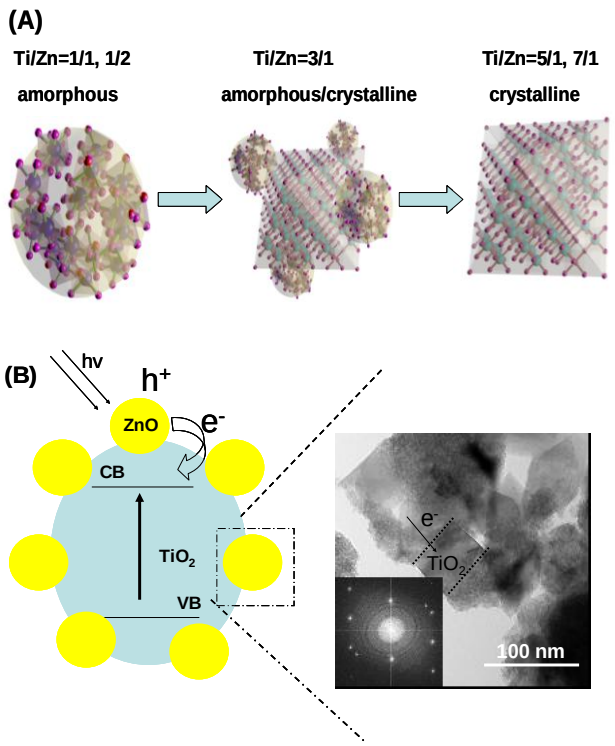

Figure 6. (A)Brief model for the structure of the ZnO/TiO_2 heterostructures with various Zn/Ti ratio; (B)A configuration model of HTZ3 consisting of TiO_2 with high crystallinity decorated with amorphous ZnO. A TEM image of the interface between crystalline TiO_2 and amorphous ZnO is also shown.

IV. Conclusions

We have successfully synthesized a novel kind of amorphous ZnO/TiO_2 composite NPs by a low-temperature hydrothermal method. The XRD and HRTEM prove that only when the mole ratio of Zn to Ti is 1/3 can obtain the amorphous ZnO/TiO_2 composite catalyst, revealing the crystallization of the ZnO/TiO_2 composite NPs depend strongly on the addition of Zn/Ti ratio.The encouraging finding could be expanded to other system or reactions and could open up a new direction in catalysis. In addition, as catalysts, these amorphous ZnO/TiO_2 composite NPs could be used for optical, magnetic, and electrical applications.

Acknowledgements

The present work is supported by "Youth Scholar Backbone Supporting Plan of General Colleges and Universities" (1253G059).

Reference

[1] A. Fujishima, K. Honda, Nature 238 (1972) 37-38.
[2] K. Lee, D. Kim, P. Roy, I. Paramasivam, B. I. Birajdar, E. Spiecker, P. Schmuki, J. Am. Chem. Soc. 132 (2010) 1478-1479.
[3] Z. Song, Q. Li, J. Mater. Sci. Technol. 13 (1997) 321-323.
[4] J. Wang, D.N. Tafen, J.P. Lewis, Z.L. Hong, A. Manivannan, M.J. Zhi, M. Li, N.Q. Wu, J. Am. Chem. Soc. 131 (2009) 12290-12297.
[5] L.X. Yang, S.L. Luo, Y. Li, Y. Xiao, Q. Kang, Q.Y. Cai, Environ. Sci. Technol. 44 (2010) 7641–7646.
[6] S. Kim, B. Fisher, H.J. Eisler, M. Bawendi, J. Am. Chem. Soc. 125 (2003) 11466-11467.
[7] I. Lee, J.B. Joo, Y.D. Yin, F. Zaera, Angew. Chem. Int. Ed. 50 (2011) 10208-10211.
[8] Y.H. Zhou, X.Y. Li, X.L. Pan, X.H. Bao, J. Mater. Chem. 22 (2012) 14155-14159.
[9] X.W. Wang, G. Liu, G.Q. Lu, H.M. Cheng, Int. J. Hydrogen Energy 35 (2010) 8199–8205.
[10] X.B. Zhang, J.M. Yan, S. Han, H. Shioyama, Q. Xu, J. Am. Chem. Soc. 131 (2009) 2778-2779.
[11] Y.J. Chen, P. Gao, R.X. Wang, C.L. Zhu, L.J. Wang, M.S. Cao, H.B. Jin, J. Phys. Chem. C 113 (2009) 10061-10064.
[12] J.M. Yan, X.B. Zhang, S. Han, H. Shioyama, Q. Xu, Angew. Chem. Int. Ed. 47 (2008)2287-2289.
[13] L.F. Cui, R. Ruffo, C.K. Chan, H.L. Peng and Y. Cui, Nanoletters, 9 (2009) 491-495.
[14] X.B. Zhang, J.M. Yan, S. Han, H. Shioyama, Q. Xu, J. Am. Chem. Soc. 131 (2009) 2778-2779.
[15] Y.J. Chen, P. Gao, R.X. Wang, C.L. Zhu, L.J. Wang, M.S. Cao, H.B. Jin, J. Phys. Chem. C 113 (2009) 10061-10064.
[16] X.B. Meng, D.S. Geng, J. Liu, M.N. Banis, Y. Zhang, R.Y. Li, X.L. Sun, J. Phys. Chem. C 114 (2010) 18330-18337.